# Noradrenaline and a Thiol Analogue on Gold Surfaces : An Infrared Reflection-Absorption Spectroscopy , X-ray Photoelectron Spectroscopy , and Near-Edge X-ray Absorption Fine Struct...

**ARTICLE** *in* THE JOURNAL OF PHYSICAL CHEMISTRY C · JANUARY 2011

Impact Factor: 4.77 · DOI: 10.1021/jp105696j

# Noradrenaline and a Thiol Analogue on Gold Surfaces: An Infrared Reflection−Absorption Spectroscopy, X-ray Photoelectron Spectroscopy, and Near-Edge X-ray Absorption Fine Structure Spectroscopy Study

**Cecilia Vahlberg, Mathieu Linares, Sebastien Villaume, Patrick Norman, and Kajsa Uvdal***

*The Division of Molecular Surface Physics and Nano Science and Division of Computational Physics, Department of Physics, Chemistry and Biology (IFM), Linköping University, SE-581 83 Linköping, Sweden*

*Received: June 21, 2010; Revised Manuscript Received: November 2, 2010*

Self-assembled monolayers and multilayers of a noradrenaline analogue (Nor-Pt) on gold substrates as well as multilayers of noradrenaline have been investigated by means of the molecular orientation, the molecule−surface interaction, the molecular composition and the functional group availability for further biointeraction processes, using X-ray photoelectron spectroscopy (XPS), infrared reflection−absorption spectroscopy (IRAS), and near-edge X-ray absorption fine structure (NEXAFS) spectroscopy. A chemical shift (1.7 eV) of the S 2p peak to lower binding energies is observed, in the XPS spectrum, indicating that the Nor-Pt molecules are chemisorbed onto the gold substrate. The IR results show that Nor-Pt adsorbate has the C═O stretching vibration modes parallel oriented relative to the gold substrate. The average tilt angle of the aromatic ring relative to the gold surface normal is determined to be approximately 51°, based on the NEXAFS measurements on Nor-Pt monolayers. The experimental results and assignments are supported with theoretical studies where we use the building block principle in the spectral analysis and compare with the measurements of noradrenaline and Nor-Pt. The theoretical calculations are shown to be useful; for angle dependence NEXAFS studies as resonances with fully $\pi^*$ or $\sigma^*$ character are preferred for correct analysis.

## 1. Introduction

Molecular design with the aim to mimic a naturally existing biological mechanism for recognition processes has emerged as a research field during the past decade. Successful biofunctionalization requires understanding on the molecular level of the complex network of chemical and biological reactions that take place for example at a solid−liquid interface or during cell signaling and in the antibody−antigen binding. To mimic such advanced and sophisticated reactions and responses in the laboratory, it becomes important to construct well-designed model systems. One way to create well-defined and highly ordered structures with a high degree of reproducibility is to use self-assembled monolayers (SAMs) for surface functionalization.[1−3]

Noradrenaline, a catecholamine derived from the amino acid tyrosine, is important both as a neurotransmitter and as a hormone, and it is an active component both in the central (brain stem, cerebral cortex, and hypothalamus) and the peripheral (postganglionic sympatic endings) nervous system. Noradrenaline interacts with and binds to adrenergic receptors ($\alpha_1$, $\alpha_2$, $\beta_1$, $\beta_2$, and $\beta_3$). These receptors belong to one of the largest families of membrane bound receptors, the so-called G-protein coupled receptors (GPCRs). Noradrenaline is active in the cell signaling process and influences a large variety of organs as the eyes, the lungs, the heart, the arterioles, the veins, the stomach, and intestine.[4]

Biofunctionalization using neurotransmitters is a new research area, which holds the promise of a multitude of technical and medical applications.[5−9]

We consider the immobilization of neurotransmitters by chemisorption to surfaces with the aim to create model systems for the development of technologies to accomplish molecular recognition and drug screening. In previous work, we have presented investigations on a tyrosine and a dopamine analogue.[10−12] Both of these molecules form well-oriented molecular structures on gold surfaces. We now continue this line of work with a study of a noradrenaline analogue (Nor-Pt). The structure formula is shown in Figure 1. Nor-Pt is obtained by the linking of noradrenaline to a thiol (mercaptopropionic acid, MPA) through an amide bond. Nor-Pt is thereafter immobilized by adsorption to gold surfaces through thiol chemistry. In this work, we are studying noradrenaline and Nor-Pt multilayers and Nor-Pt adsorbed on gold using X-ray photoelectron spectroscopy (XPS), infrared reflection−absorption spectroscopy (IRAS), and near-edge X-ray absorption fine structure (NEXAFS) spectroscopy to characterize the electronic and molecular structures and to address issues as the chemical composition, the binding strength to the gold substrate, and the molecular orientation relative to the gold surface.

Spectral assignments are made with aid of a molecular building block principle to pinpoint specific spectral features to specific fragments, or functional groups, of the molecules. The experimental results and assignments are supported with theoretical calculations. In the theoretical work, we consider Nor-Pt and noradrenaline in line with the experimental studies, and also 3,4-dihydroxytoluene and 2-hydroxyethyl-3-mercaptoamide (see Figure 1) to enable detailed assignments.

## 2. Materials and Methods

**2.1. Substrate Preparation and Monolayer Formation.** The gold substrates used in this study were prepared by gold evaporation using an electron beam evaporation system onto clean, single-crystal silicon (100) wafers at a rate of ∼10 Å/s. The silicon wafers were primed with a 25 Å thick titanium layer, at a rate of ∼2 Å/s before the gold evaporation. The base pressure

* Corresponding author. Fax: 46-13-137-568. E-mail: kajsa@ifm.liu.se.

10.1021/jp105696j 
Published on Web 12/13/2010

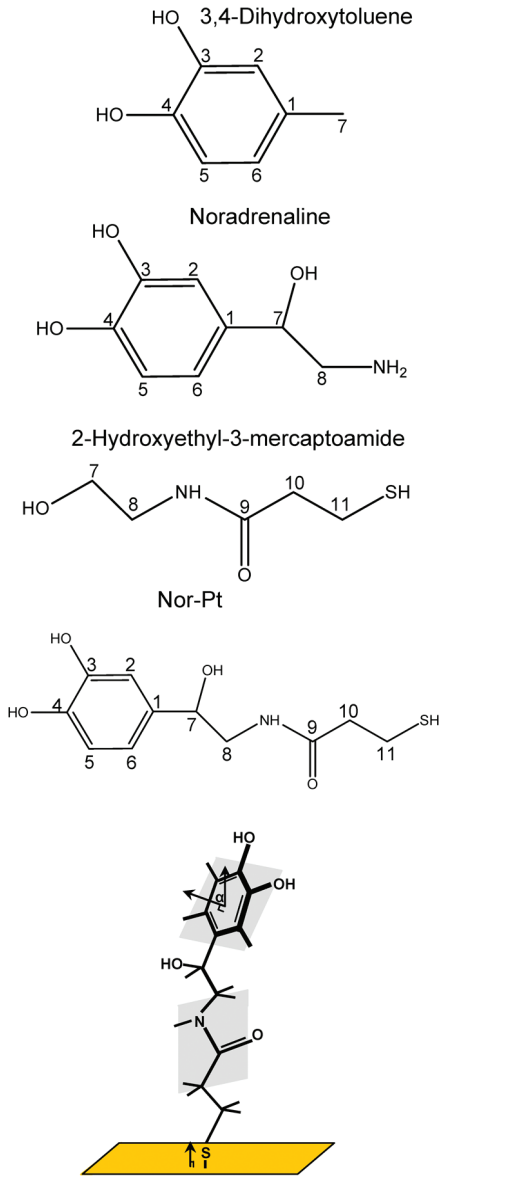


**Figure 1.** Molecular structures with numbering of carbon atoms for 3,4-dihydroxytoluene, noradrenaline, 2-hydroxyethyl-3-mercaptoamide, and Nor-Pt. The lower illustration depicts Nor-Pt adsorbed to a gold surface with α defined as the angle between the surface normal and the normal of the plane spanned by the aromatic ring.

was approximately $5 \times 10^{-9}$ Torr and the evaporation pressure approximately $2 \times 10^{-7}$ Torr. The gold surfaces were, prior to incubation in the Nor-Pt solution, cleaned in a basic peroxide solution (Milli-Q water:$NH_3$(25%):$H_2O_2$(28%), 5:1:1) for about 10 min at 80 °C, to remove organic contaminations, and then rinsed carefully with Milli-Q water. Noradrenaline and Nor-Pt were dissolved in ethanol. The concentration of the Nor-Pt incubation solution was 0.5 mM, and the incubation was done at room temperature. The incubation solution was kept in darkness, due to the sensitivity of light. The incubation time was <24 h, to avoid formation of overlayers. After incubation, the gold surfaces were rinsed three times in ethanol, ultrasonicated for 15 min in ethanol, rinsed three times again, and thereafter dried in nitrogen gas. The surfaces were immediately placed in the instruments after drying. The multilayer samples were prepared by drying droplets of molecular solution onto gold surfaces for the XPS and NEXAFS measurements and a $CaF_2$ window for the transmission infrared spectroscopy measurements. The molecular weight of noradrenaline is 169.18 g/mol, and the molecular weight of Nor-Pt is 257.31 g/mol. The molecular length of noradrenaline is ∼8 Å, and the molecular length of Nor-Pt is ∼12 Å.

**2.2. X-ray Photoelectron Spectroscopy.** XPS core level spectra of Nor-Pt and noradrenaline were recorded on a VG spectrometer, with a CLAM2 analyzer, using Mg Kα photons (1253.6 eV). The power of the X-ray gun was 300 W. The C 1s core level spectra were based upon photoelectrons with a takeoff angle of 30° with respect to the surface normal. High-resolution XPS measurements were performed at beamline D1011 at the MAX II synchrotron storage ring at MAX-Lab in Lund, Sweden. The spectra were recorded with a Scienta SES 200 analyzer. The high-resolution XPS core level S 2p spectrum was recorded using a photon energy of 260 eV and a pass energy of 50 eV. The measurement was based on photoelectrons with a takeoff angle of 0° with respect to the normal of the surface. The monolayer Nor-Pt spectrum was aligned using the Au ($4f_{7/2}$) peak positioned at 84.0 eV. The multilayer noradrenaline spectrum was aligned using the binding energy position of 284.3 eV for the C (2p) peak corresponding to aromatic carbon. Curve fitting was done using the XPSPEAK95 program (version 2.0) using a Gaussian−Lorentzian function with an 80:20 ratio.

**2.3. Near-Edge X-ray Absorption Fine Structure Spectroscopy.** The NEXAFS measurements were performed at beamline D1011 at MAX-Lab (see section 2.2). The spectra were carried out at the C 1s absorption edge using partial electron yield (PEY) detection, using a multichannel plate detector. The retardation voltage was set to −150 V. The energy resolution is ∼0.2 eV. An incidence angle of the synchrotron light of 55° was used for the multilayers of noradrenaline and Nor-Pt. Two different incidence angles of the synchrotron light, 90° (**E**-vector parallel to the gold surface) and 10° (**E**-vector near surface normal), were used to investigate the orientation of Nor-Pt adsorbed onto the gold surfaces. The raw NEXAFS spectra were normalized by division of the corresponding NEXAFS spectrum of a sputtered clean gold substrate, to correct for monochromator structures and the detector response.

**2.4. Infrared Spectroscopy, Ellipsometry, and Contact Angle Goniometry.** The infrared reflection−absorption (RA) spectra were recorded on a Fourier transform spectrometer, Bruker, model IFS66. The spectrometer is equipped with a grazing angle of incidence reflection accessory aligned at 85° and a mercury cadmium telluride (MCT) detector. Liquid nitrogen was used to cool the detector before the measurements. A three-term Blackmann-Harris apodization function is applied to the interferograms before Fourier transformation. The transmission (TR) spectra of Noradrenaline and Nor-Pt were recorded on a Vertex 70 instrument. The resolution for the IRAS and the transmission IR measurements was 2 $cm^{-1}$. Both measurement chambers were continuously purged with nitrogen gas before and during the measurements, to reduce the contribution of water and carbon dioxide. The thickness of the self-assembled monolayer of the Nor-Pt molecule adsorbed onto the gold substrate was measured using single wavelength ($\lambda = 632.8$ nm) null ellipsometry. The measurements were performed on an automatic Rudolph Research AutoEl ellipsometer equipped with a He−Ne laser light source. The angle of incidence is 70°. All measurements were performed in air. The static contact angle measurements of water, on the Nor-Pt self-assembly, were performed using a CAM 200 goniometer.

**2.5. Theoretical Calculations.** Theoretical calculations were carried out for the determination of ionization potentials and NEXAFS spectra, both regarding the carbon *K*-edge, and IR spectra. All calculations were made for isolated molecules at

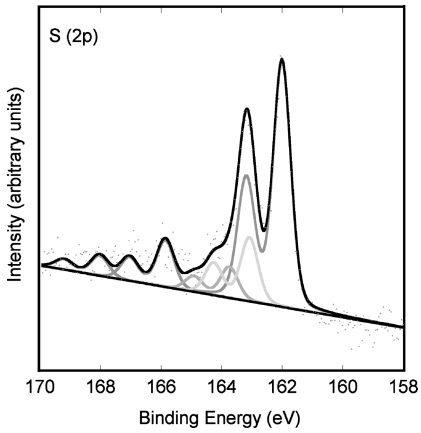


**Figure 2.** S 2p core level XPS spectrum of Nor-Pt on a gold surface. The experimental spectrum (dots) is shown together with curve fittings (solid black and gray).

the respective ground-state equilibrium geometries, as determined with use of density functional theory (DFT) in conjunction with the B3LYP exchange correlation functional[13] and Dunning's cc-pVTZ family of basis sets.[14] The IR spectra were obtained in the harmonic force field approximation based on analytic molecular Hessians at the B3LYP/cc-pVTZ level of theory. The frequencies have been scaled by 0.97. Ionization energies were obtained in the Hartree−Fock approximation by separate state optimizations of the electronic structure of the ground and core ionized states, an approach known as the ΔSCF method. Separate optimizations were made for ionized states with core holes localized to the individual carbons, and the basis set used in these calculations was chosen as cc-pVDZ. The NEXAFS spectra were determined from the imaginary part of the electric dipole polarizability, which relates to the absorption cross-section according to

$$\sigma(\omega) = \frac{4\pi\omega}{3c}\,\mathrm{Im}(\alpha_{xx} + \alpha_{yy} + \alpha_{zz}) \qquad (1)$$

The individual tensor components of the polarizability will correspond to absorption along the three Cartesian molecular axes and, hence, provide the polarization dependence in the spectrum. Calculations of the polarizability are done with the complex polarization propagator approach[15,16] in the DFT approximation, which is to be understood as time-dependent DFT with inclusion made of relaxation due to the finite lifetime of the excited states. Proper long-range Coulomb interaction between the hole and the electronic state in the absorption process is achieved by use of the Coulomb attenuated method B3LYP (CAM-B3LYP) functional with parameters $\alpha = 0.19$, $\beta = 0.81$, and $\mu = 0.33$. In these calculations we employed the augmented cc-pVDZ (aug-cc-pVDZ) basis set which is suitable for a description of valence (but not Rydberg) transitions. Geometry optimizations and IR frequency calculations were carried out with the Gaussian program,[17] whereas calculations of X-ray absorption properties were done with the Dalton program.[18]

## 3. Results and Discussion

**3.1. X-ray Photoelectron Spectroscopy.** XPS is an excellent technique to study the electronic structure of thin organic films, the chemical composition, and the molecular orientation as well as the molecule−surface interaction. The S 2p core level XPS spectrum of a monolayer of Nor-Pt is shown in Figure 2. There is a strong double peak, with the individual peaks found at binding energy positions of 162.0 and 163.2 eV. The two peak areas have a relative ratio of 2:1. The double peak feature is clearly observed and corresponds to spin−orbit splitting.[19] The individual peaks are assigned to $2p_{3/2}$ and $2p_{1/2}$, respectively. This S 2p double peak is assigned to chemisorbed sulfur atoms, in good agreement with earlier published data.[10−12,20,21] The binding energy position is characteristic for sulfur species chemically bonded to gold substrates as thiolate species.[10−12,20,21] There is a low-intensity S 2p double peak with $2p_{3/2}$ and $2p_{1/2}$ binding energy peak positions found at 163.1 and 164.3 eV, respectively. We assign this double peak as possible X-ray induced sulfur species.[22−24] This is in agreement with the binding energies found for X-ray induced sulfur species for 1-dodecanethiol (C12SH)[22] and 1-octadecanethiol (C18SH)[23] on gold surfaces. Damages in SAMs due to X-ray irradiation are discussed in a recently published review article written by Zharnikov.[25] The binding energy position of the $2p_{3/2}$ peak is found at lower binding energies than in the case of unbound thiols and disulfides, which is found at binding energies between 163.5 and 164 eV.[20,21] The small double peak, with the $2p_{3/2}$ and $2p_{1/2}$ binding energy positions found at approximately 163.7 and 164.9 eV, respectively, is assigned to unbound sulfur species.[21,26−28] These binding energies are in good agreement with what Castner et al.[21] have found for unbound thiols (-SH) and also with what we have found for multilayers of L-cystein[27] and multilayers of a peptide[28] on gold substrates. There are also spectral features with low intensity detected at about 166−168 eV, which we assign to oxidized sulfur ($-SO_x$), consistent with earlier published data.[29−32]

The core level C 1s XPS spectra of a multilayer of noradrenaline and of Nor-Pt adsorbed onto a gold surface is shown in Figure 3A,B, respectively. A curve fit to the experimental data is done. The presence of chemical groups is assumed, on the basis of the chemical structure of noradrenaline and Nor-Pt, with binding energy peak positions chosen consistent with data earlier presented in the literature. The line shape of the C 1s spectra is broad, and we have made tentative assignments.

Two peaks of almost equal intensity are visible in the noradrenaline experimental spectrum; see Figure 3A. The peak positioned at 284.3 eV was assigned to the four aromatic carbons (labeled 1, 2, 5, and 6 in Figure 1), which is in agreement with the interpretation of related molecules with aromatic ring structures as multilayers of tyrosine[33] as well as benzenethiol adsorbates on gold surfaces.[34] Further support for this assignment is also provided by our previous study on the closely related system TPT (a tyrosine analogue) adsorbed on gold.[11] The peak at the high binding energy side, positioned at about 286 eV, is suggested to consist of several components with slightly different binding energies, which is also used in the curve fitting procedure. The peak at about 285.8 eV is assigned as hydroxyl carbons in the aromatic ring (carbons 3 and 4 in Figure 1), the peak at about 286.2 eV is assigned as the amine carbon (carbon 8, see Figure 1), and the peak at 286.5 eV is assigned as the hydroxyl carbon (carbon 7, see Figure 1). The assignments, for these binding energy positions, are in agreement with the literature,[35−38] for example the study of immobilized peptides on $TiO_2$ surfaces done by Iucci et al.[35] and the work of alkanethiol terminated with a catechol group reported by Simmons et al.[36] The low broad structure at the high binding energy side, at about 290 eV, is assigned to shakeup satellites for the aromatic carbons[39] and possibly contaminations. The small peak, positioned at 287.7 eV, is assigned as quinone carbons,[40] as noradrenaline is easily oxidized

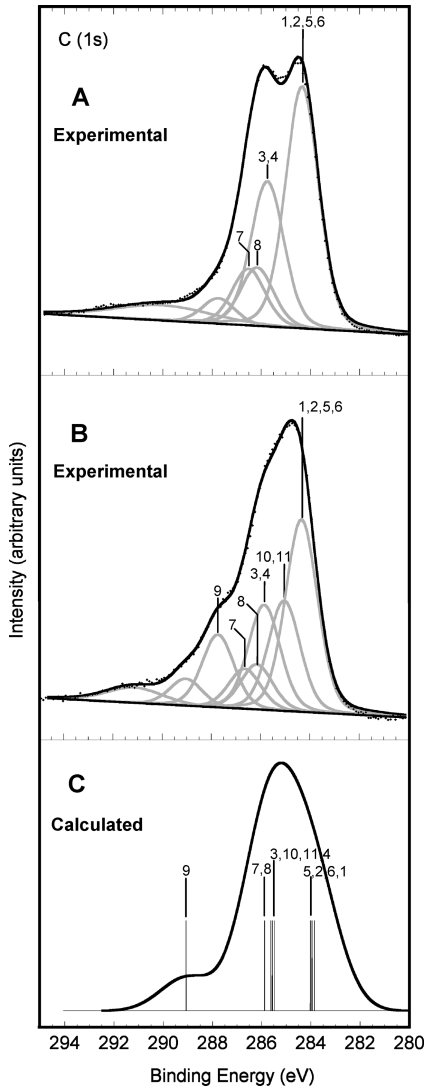


**Figure 3.** C 1s core level XPS spectra of (A) a multilayer of noradrenaline, (B) the monolayer of Nor-Pt adsorbed on a gold surface, and (C) isolated Nor-Pt. Panels A and B refer to experimental results, and panel C refers to ΔSCF calculations.

by molecular oxygen.[41] The XPS C 1s core level spectrum of Nor-Pt adsorbed onto a gold surface is presented in Figure 3B. A large peak with several shoulders is observed in the spectrum. We assign the peak at 284.3 eV, to the aromatic carbons. The peak with the binding energy position at 285.0 eV is assigned to the aliphatic carbons[44] and the peak with the binding energy position at 285.9 eV as hydroxyl carbons present in the aromatic ring. The peaks with the binding energy positions 286.2 and 286.6 eV are assigned to the carbon attached to the amide group and the hydroxyl carbon, respectively (carbons 8 and 7, see Figure 1). The shoulder on the high binding energy side, at 287.7 eV, is assigned as the carbon present in the amide moiety, which is also in agreement with results reported in the literature.[42] In the presence of oxygen, oxidation of hydroxyl groups in the aromatic ring is possible.[41] We suggest oxidation of a small fraction of the hydroxyl groups present in the ring structure has occurred, resulting in quinone formation,[40] in agreement with our XPS assignment of the noradrenaline multilayer spectrum. The shakeup line for the aromatic carbons and possibly contaminations was positioned at approximately 291 eV. A small unexpected peak, located at 289.0 eV is also present in the spectrum, which we assign as carbon present in a carboxylic acid group.[43]

**TABLE 1: Relative Intensities of Multilayers of Noradrenaline and Nor-Pt as Well as Relative Intensities for Nor-Pt Monolayers as a Function of Increasing Takeoff Angles**

| | C/N | S/N | O/N | C/S | O/S |
|---|---|---|---|---|---|
| noradrenaline[a] | 8.0 | | 3.0 | | |
| noradrenaline multilayer[b] | 8.4 | | 3.1 | | |
| Nor-Pt[a] | 11.0 | 1.0 | 4.0 | 11.0 | 4.0 |
| Nor-Pt multilayer[b] | 17.2 | 1.1 | 3.7 | 15.7 | 3.4 |
| Nor-Pt monolayer bulk mode[c] (TOA = 30°) | 13.1 | 0.8 | 4.3 | 16.3 | 5.4 |
| Nor-Pt monolayer surface mode[c] (TOA = 80°) | 14.8 | 0.8 | 4.9 | 18.7 | 6.2 |

[a] The stoichiometric ratio for Nor-Pt and noradrenaline based on the molecular structure. [b] The experimental relative intensities obtained from the XPS measurements of a multilayer of noradrenaline and Nor-Pt. [c] Relative intensities for a monolayer of Nor-Pt in bulk and surface sensitive mode.

Further support of this assignment is that IR vibrational lines associated with a -COOH functional group is detected in the TR spectrum of Nor-Pt (Figure 5B) at approximately 1740 $cm^{-1}$.[45] This small contamination could be traces of MPA used during the synthesis of Nor-Pt.

Relative intensities between the elemental peaks (C 1s, O 1s, N 1s, and S 2p), from Nor-Pt and noradrenaline, are presented in Table 1. The stoichiometric values are calculated on the basis of the molecular structure of noradrenaline and Nor-Pt. The relative intensities for the multilayers, if randomly organized, are expected to be close to the stoichiometric values. The relative ratios measured for noradrenaline are close to the stoichiometric values. In the case of multilayers of Nor-Pt, the relative ratios measured for C 1s are larger than the stoichiometric values. We suggest that these contaminations originate from the synthesis. In the case of monolayers, information regarding the molecular orientation can be obtained when comparing the relative intensities from different takeoff angles. The C 1s/S 2p and O 1s/S 2p ratios for the surface mode measurement (TOA = 80°) is higher than the ratios for the bulk mode measurement (TOA = 30°). These results indicate that the sulfur atoms are oriented close to the gold substrate compared to the carbon and oxygen atoms.

We have conducted theoretical calculations of core ionization potentials (IPs), on the basis of the ΔSCF approach to further support the assignments of Nor-Pt. The theoretical spectrum is shown in Figure 3C, in which bars are used to mark the obtained IPs, and Gaussian broadenings have been used to mimic the XPS spectrum of Nor-Pt (Figure 3B). The energy scale of the theoretical spectrum was shifted 8.0 eV, to be aligned with experimental spectrum. On the basis of the theoretical calculations, we suggest that the core level XPS binding energy peak at around 284 eV should be assigned as aromatic carbons. This binding energy peak is separated by 1.5−2.0 eV from the peaks assigned as the hydroxyl, aliphatic, and amine carbons. The binding energy peak at approximately 289 eV is assigned as the carbonyl carbon present in the amide moiety.

**3.2. Infrared Spectroscopy.** One aim of the present study is to determine the molecular orientation of Nor-Pt when adsorbed onto a gold substrate. Infrared reflection−absorption and transmission (TR) spectroscopies were used as complement to XPS and NEXAFS in order to address this issue. The IRAS absorption bands follow the surface dipole selection rule. Consequently, only molecular vibrational modes with transition dipole moment vectors aligned parallel to the surface normal can be observed in these spectra.[46] IRAS measurements, on a

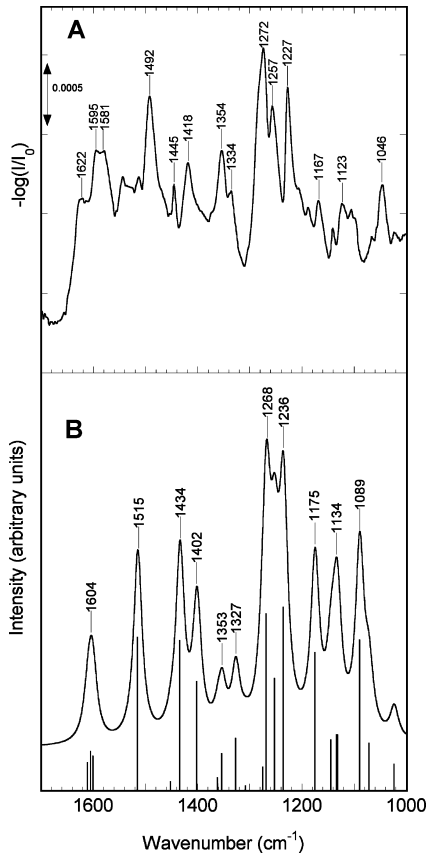


**Figure 4.** IR spectra of noradrenaline: (A) experimental spectrum recorded in transmission mode and (B) theoretical spectrum obtained at the DFT/B3LYP/cc-pVTZ level of theory.

monolayer of Nor-Pt adsorbed onto a gold surface, are done as well as TR measurements on Nor-Pt multilayers. We also performed TR measurements on a multilayer of noradrenaline. This is done to investigate details and to strengthen the assignments made for Nor-Pt. Theoretical calculations of frequencies and intensities in the harmonic field approximation were performed to further support the assignments of the experimental spectra of multilayers of noradrenaline and Nor-Pt. The experimental TR and theoretical spectra of noradrenaline are shown in Figure 4A,B, respectively. There are many vibrational modes that contribute to the same vibration bands, which can be observed in the detailed summary of the assignment, presented in Table 2. Characteristic bands from symmetric C−C stretching vibrational modes of the aromatic ring were located at 1622 and 1581 $cm^{-1}$.[47,48] The asymmetric C−C stretching vibrational modes of the aromatic ring were found at 1492 and 1445 $cm^{-1}$.[47,48] The vibration band located at 1492 $cm^{-1}$ has the highest intensity of the four bands assigned to aromatic stretching vibrational modes. Aromatic ring vibrational modes also contribute to seven bands in the 1000−1360 $cm^{-1}$ region. The band found at 1595 $cm^{-1}$ is assigned to the scissoring vibrational mode in the amino group.[49] The vibration bands at 1418 and 1257 $cm^{-1}$ are assigned to O−H bending vibrational modes.

The experimental RA and TR spectra together with the theoretical IR spectrum of Nor-Pt are shown in Figure 5A−C. A detailed summary of peak assignments is presented in Table 3. Our assignments have been based on a combination of results in the literature for molecules with similar functional groups together with theoretical calculations as well as the results presented above for noradrenaline.

Two vibrational bands located at 1547 and at 1604 $cm^{-1}$ are observed in the TR spectrum and at 1550 and 1615 $cm^{-1}$ in the RA spectrum. We assign these vibrational bands to the C−C stretching mode of the aromatic ring. Aromatic ring vibrational modes also contribute to five bands found in the 1000−1450 $cm^{-1}$ region in both the RA and TR spectra. The vibration bands found at 1642 and at 1656 $cm^{-1}$ in the TR and RA spectra, respectively, are assigned to the stretching mode of the C═O bond present in the amide moiety. This vibrational band is commonly noted as the amide I absorption

**TABLE 2: Proposed IR Assignment of Noradrenaline[a]**

| experimental $\upsilon$ ($cm^{-1}$) $CaF_2$ tablet (TR) | theoretical $\upsilon$ ($cm^{-1}$) | theoretical intensity | assignment |
|---|---|---|---|
| 1622 | 1611 | 19 | Ar C−C sym. stretching |
| 1595 | 1605 | 26 | $NH_2$ scissoring |
| 1581 | 1600 | 23 | Ar C−C sym. stretching |
| 1492 | 1515 | 104 | Ar C−C asym. stretching |
| 1445 | 1434 | 102 | Ar C−C asym. stretching |
| 1418 | 1402 | 74 | O−H bending |
| 1354 | 1353 | 25 | $CH_2$ wagging + O−H bending + Ar O−H bending |
| 1334 | 1327 | 35 | Ar C−H bending + Ar O−H bending + O−H bending + C−H bending |
| 1272 | 1275 | 16 | $CH_2$ twisting + $NH_2$ bending |
| | 1268 | 120 | Ar breathing + O−H bending |
| 1257 | 1253 | 76 | O−H bending |
| 1227 | 1236 | 125 | Ar O−H stretching |
| 1167 | 1175 | 94 | Ar C−H bending + Ar O−H bending |
| 1123 | 1144 | 34 | Ar C−H bending + Ar O−H bending + $CH_2$ bending + $NH_2$ bending |
| | 1134 | 38 | Ar C−H bending + C−O streching + $CH_2$ bending + $NH_2$ bending |
| | 1132 | 38 | Ar C−H bending + Ar O−H bending + $CH_2$ bending + $NH_2$ bending |
| 1046 | 1089 | 103 | Ar O−H bending + Ar C−H bending |
| | 1072 | 32 | C−O stretching |
| | 1023 | 18 | C−N stretching |

[a] The measurements were done on multilayers of noradrenaline on a $CaF_2$ window (TR). The experimental measurements were supported with theoretical calculations.

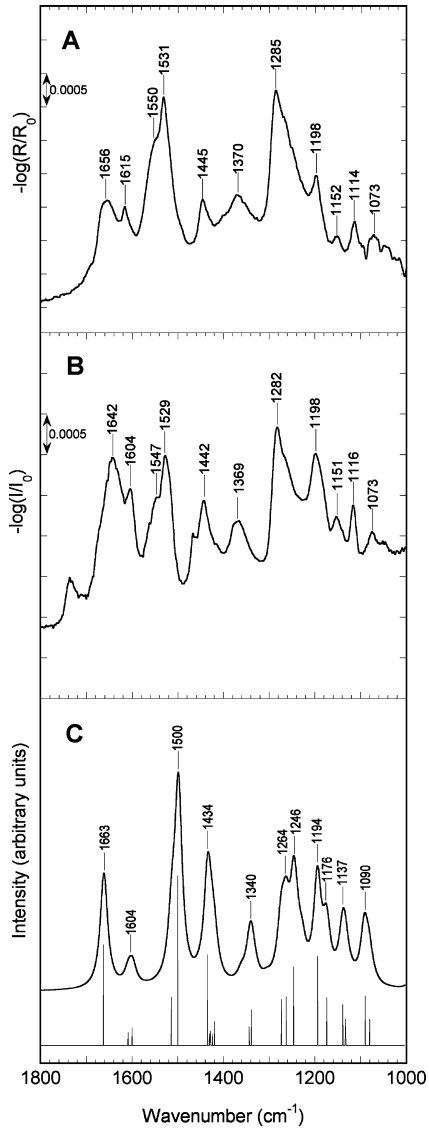


**Figure 5.** IR spectra of Nor-Pt: (A) experimental spectrum of surface adsorbate recorded in reflection mode, (B) experimental spectrum of multilayers of Nor-Pt recorded in transmission mode, and (C) theoretical spectrum obtained at the DFT/B3LYP/cc-pVTZ level of theory.

band.[50] This band is prominent in the TR spectrum but weak in the RA spectrum, which, due to the so-called surface selection rule,[46] indicate that the main component of the C═O bond vibration modes is oriented parallel to the plane of the gold surface. The absorption bands found at 1529 and 1531 $cm^{-1}$ in the TR and RA spectra, respectively, are assigned to the C−N stretching mode in the amide moiety. This vibration is often called the amide II vibration band. The two absorption bands located at 1530 and approximately 1550 $cm^{-1}$ have been assigned to amide II and C−C stretching of the aromatic ring, respectively.[48] There are, however, also alternative assignments for these vibrational modes found in the literature.[47] In this paper, we have done a thorough experimental study supported by calculations with focus on this issue. We carried out a full set of TR measurements on mixed solutions as a function of concentration ratios of noradrenaline and Nor-Pt. The results are shown in Figure 6. It is obvious that when comparing the intensity of the two vibration bands in questions, the peak located at approximately 1530 $cm^{-1}$ becomes more pronounced when the amount of Nor-Pt increases relative to the amount of noradrenaline present in the sample. Our conclusion is that, in this case, the peak located at approximately 1530 $cm^{-1}$ does indeed correspond to vibrational modes in the amide moiety and consequently the peak located at 1550 $cm^{-1}$ is to be associated mainly with vibrational modes in the aromatic ring. Vibrational modes in the amide moiety also contribute to bands found at about 1370 and at 1198 $cm^{-1}$ in both the TR and the RA spectra. The vibration band at about 1740 $cm^{-1}$ in the TR spectrum is assigned as the C═O stretching vibrational mode in a carboxylic acid; thus, there is a small amount of contamination observed, consistent with the XPS results. Many of the vibration bands in the spectra, of both noradrenaline and Nor-Pt, have contributions from the aromatic ring vibrational modes. Vibrational modes from the amide moiety give characteristic bands, which could be clearly observed in the Nor-Pt spectra.

Three different incubation times were used for the ellipsometry and contact angle measurements. The thickness, for the Nor-Pt self-assembly, after 8, 24, and 48 h incubation were 15.1 ± 0.7, 15.0 ± 0.4, and 15.6 ± 1.0 Å, respectively. The static contact angle of water, on the Nor-Pt monolayer, after 8, 24, and 48 h incubation were <17, <15, and <15°, respectively.

**3.3. Near-Edge X-ray Absorption Fine Structure Spectroscopy.** NEXAFS is a useful technique in studies of molecular orientation, identification and orientation of functional groups as well as investigation of intramolecular bonds.[51] Carbon *K*-edge spectra of multilayers of noradrenaline, multilayers of Nor-Pt, and monolayers of Nor-Pt on a gold substrate are presented in Figures 7−9. A summary of the peak assignments are presented in Table 4.

The C *K*-edge spectrum of multilayers of noradrenaline is presented in Figure 7 as well as an experimental and a theoretical blow-up spectrum showing region 284−290 eV. Parts of the theoretical spectrum has been published in *Chirality* by Villaume and Norman.[52] The assignments are done on the basis of the theoretical calculations as well as published NEXAFS data on related molecular systems. There is a strong resonance structure observed at a photon energy of approximately 285 eV. We assign this peak as C 1s to $\pi^*$ transitions of the aromatic carbons. There is a broadening of this peak because of differences in the chemical environment of carbons 2, 5, and 6 compared to carbon 1; see the structural formula in Figure 1. This is consistent with NEXAFS studies reported on phenylalanine and tyrosine multilayers and also with our previously published studies on a tyrosine and a dopamine analogue on gold surfaces.[11,12,33,53] The resonance observed at a photon energy of 286.7 eV corresponds predominantly to aromatic C 1s (C−OH) to $\pi^*$ transitions (the carbons labeled 3 and 4 in Figure 1).[11,12,33,53] The peak, found at 288.1 eV, we consider as contribution from $\pi^*$(C═O) transitions in quinones[54] (see the discussion in section 3.1). The resonance located at about 290 eV is attributed to C 1s to $\sigma^*$(C−OH) and $\sigma^*$(C−N) transitions.[55] We assign the broad features located at approximately 294 eV to $\sigma^*$(C−C) and $\sigma^*$(C−N) transitions.[56] The broad peak located at about 303 eV is assigned to $\sigma^*$(C═C) and $\sigma^*$(C═O) transitions.[11,12,56]

The carbon *K*-edge spectrum of multilayers of Nor-Pt is shown in Figure 8 as well as an experimental and a theoretical blow-up spectrum (region 284−290 eV). The first resonance, at about 285 eV, is assigned as C 1s to $\pi^*$ transitions of the aromatic carbons, consistent with the results for multilayers of noradrenaline.[11,12,33,53] This peak has an asymmetric broadening due to a different chemical environment, i.e., different nearest

**TABLE 3: Proposed IR Peak Assignment of Nor-Pt[a]**

| experimental $\upsilon$ ($cm^{-1}$) | | theoretical | | |
|---|---|---|---|---|
| Au (RA) | $CaF_2$ tablet (TR) | $\upsilon$ ($cm^{-1}$) | intensity | assignment |
| 3251 | 3300 (broad) | | | O−H str, N−H str (amide A) |
| 2936 | 2919 | | | $CH_2$ asym. stretching |
| | 2850 | | | $CH_2$ sym. stretching |
| 1656 | 1642 | 1663 | 173 | C═O stretching |
| 1615 | 1604 | 1609 | 22 | Ar C−C sym. stretching |
| | | 1600 | 30 | Ar C−C sym. stretching |
| 1550 | 1547 | 1514 | 83 | Ar C−C asym. stretching |
| 1531 | 1529 | 1500 | 292 | C−N stretching |
| 1445 | 1442 | 1435 | 156 | Ar C−C stretching + O−H bending + Ar O−H bending |
| | | 1429 | 24 | O−H bending + $CH_2$ scissoring |
| | | 1425 | 20 | O−H bending + $CH_2$ scissoring (carbon 10) |
| | | 1420 | 41 | O−H bending + $CH_2$ scissoring |
| 1370 | 1369 | 1344 | 32 | $CH_2$ wagging (carbon 10) + N−H bending |
| | | 1339 | 61 | $CH_2$ wagging (carbon 8) |
| 1285 | 1282 | 1273 | 79 | $CH_2$ twisting + Ar breathing |
| | | 1263 | 84 | $CH_2$ twisting |
| | | 1246 | 135 | O−H bending |
| 1198 | 1198 | 1194 | 153 | N−H bending + $CH_2$ wagging |
| 1152 | 1151 | 1174 | 82 | Ar C−H bending + Ar O−H bending |
| 1114 | 1116 | 1139 | 70 | Ar C−H bending + Ar O−H bending |
| | | 1133 | 45 | Ar C−H bending + C−O stretching |
| 1073 | 1073 | 1090 | 85 | Ar C−H bending + Ar C−O stretching |
| | | 1080 | 45 | C−O stretching + Ar C−H bending |

[a] The experimental measurements were done on Nor-Pt adsorbates on gold (Au(RA)) and on multilayers of Nor-Pt on a $CaF_2$ window (TR). The experimental measurements were supported with theoretical calculations.

neighbors of carbons 2, 5, and 6 compared to carbon 1. This induces chemical shifts for the corresponding peaks, just as in the case of noradrenaline. We assign the peak, located at approximately 287.1 eV, to aromatic $\pi^*$(C−OH) transitions, which is in agreement with our assignment for the multilayers of noradrenaline as well as assignments made in the literature for related analogues.[11,12,33,53] There is strong resonance located at about 287.5 eV in the multilayer Nor-Pt spectrum. The high intensity of this band indicates that the resonance is associated with $\pi^*$-transitions, and we attribute this resonance predominantly to $\pi^*$(C═O) transitions in the amide moiety. The peak at 287.5 eV may also have a small contribution from $\sigma^*$(C−S) transitions.[55] The resonance at 288.1 eV in the multilayer Nor-Pt spectrum is assigned to $\pi^*$(C═O) transitions associated with carboxyl groups and quinones.[54] It is also likely that $\pi^*$(C═C) transitions and $\sigma^*$ resonances contribute to this peak. A NEXAFS study reported by Cooper et al. on a glycyl−glycine molecule showed a chemical shift for the peaks corresponding to carbons present in an amide moiety compared to carbons present in a carboxylic acid.[57] The peak assigned to the $\pi^*$(C═ONH) transitions was located at a lower photon energy position compared to the peak assigned to the $\pi^*$(C═OOH) transitions.[57] We assign the peak located at approximately 290 eV to $\sigma^*$(C−OH) and $\sigma^*$(C−$NH_2$) transitions,[55] in agreement with our corresponding results for the noradrenaline multilayers, and the peak at 291.6 eV is assigned to $\sigma^*$(C−C) transitions. Finally, the resonances at about 293 and 303 eV are assigned to $\sigma^*$(C−C, C−N) and $\sigma^*$(C═C, C═O) transitions, respectively.[56]

Two C *K*-edge spectra of monolayers of Nor-Pt on gold substrates as well as two blow-up spectra of the absorption edge (region 290−294) are shown in Figure 9. One spectrum (solid black line) is obtained using normal incidence angle for which the angle of the beam polarization with respect to surface normal is 90° ($\theta = 90°$), and the other spectrum (solid gray line) is obtained using grazing incidence angle with $\theta = 10°$. The resonance, positioned at about 285 eV, is assigned to C 1s to $\pi^*$ transitions of the aromatic carbons (carbons labeled 1, 2, 5, and 6 in Figure 1). The broadening of the peak is due to differences in the chemical environment of carbons 2, 5, and 6 compared to carbon 1, which induces the chemical shifts. This is consistent with the results from the noradrenaline and Nor-Pt multilayers. This resonance can be used to determine the orientation of the aromatic ring with respect to the normal of the gold surface; we denote this angle by $\alpha$ (see Figure 1). The integrated peak intensity has a dependence on $\alpha$ and $\theta$ as follows:[51]

$$I(\theta, \alpha) \propto 1 + \frac{1}{2}(3\cos^2\theta - 1)(3\cos^2\alpha - 1) \qquad (2)$$

The average tilt angle of the aromatic ring can be extracted by forming the ratio of integrated band intensities between the two considered angles of incidence. For the monolayers of Nor-Pt on a gold substrate, the average tilt angle of the $\pi^*$ orbitals of the aromatic ring with respect to the surface normal was determined to be equal to 51°. There are a number of absorption bands at higher energies that can be observed in Figure 9. The resonance at 287.0 eV is assigned to aromatic carbon $\pi^*$ (C−OH) transitions, in accordance with the corresponding bands in the multilayer spectra for noradrenaline and Nor-Pt that have been discussed above. In the multilayer spectrum Nor-Pt, we assigned the strong resonance positioned at 287.5 eV as a $\pi^*$(C═O) transitions in the amide moiety. The corresponding resonance for the monolayer is observed as a shoulder positioned at approximately 287.8 eV. The peak at 288.4 eV is assigned as $\pi^*$(C═O) transitions in carboxyl moieties and quinones. Finally, the resonances at 290.6, 292, and 303 eV are attributed to $\sigma^*$(C−C), $\sigma^*$(C−C, C−N), and $\sigma^*$(C═C, C═O) transitions, respectively. We also did theoretical calculations on 3,4-dihydroxytoluene, 2-hydroxyethyl-3-mercaptoamide, the sum of 3,4-dihydroxytoluene and 2-hydroxyethyl-3-mercaptoamide, and

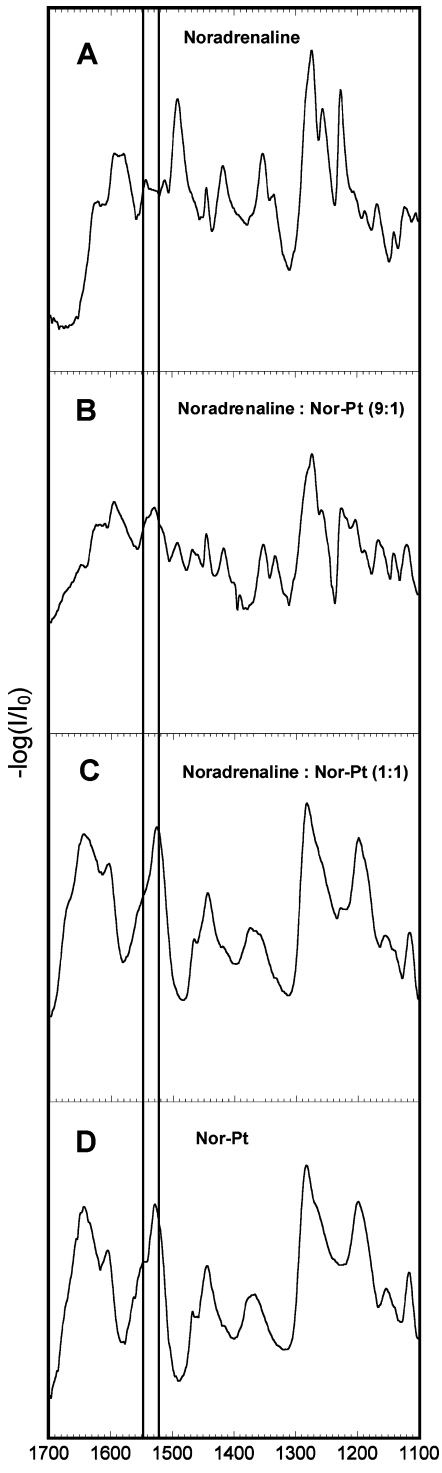


**Figure 6.** Experimental IR spectra recorded in transmission mode for samples with varying mixtures of noradrenaline and Nor-Pt: (A) pure noradrenaline, (B) 9:1 mixture, (C) 1:1 mixture, and (D) pure Nor-Pt.

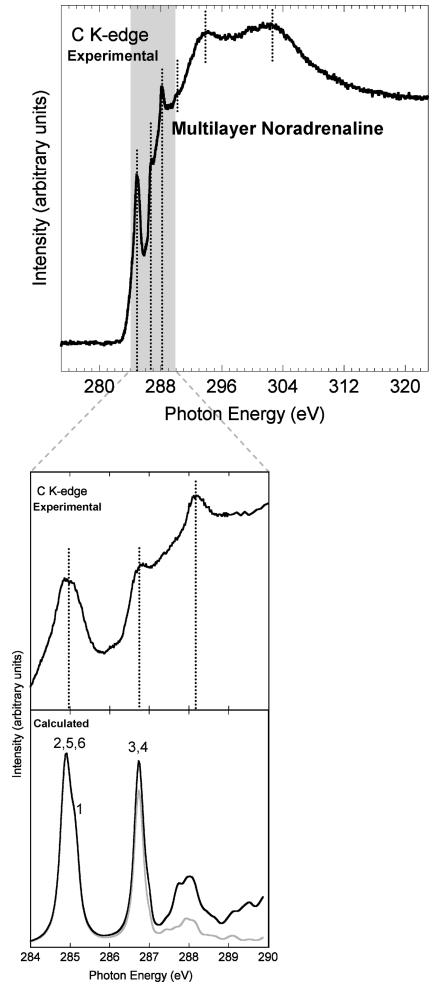


**Figure 7.** Carbon *K*-edge NEXAFS spectra of noradrenaline in a multilayer form. The experimental spectrum is measured at an angle $\theta = 55°$ (the angle between the surface normal and the beam polarization). The enlargement includes a comparison with the corresponding theoretical spectrum.[52]

Nor-Pt (see the chemical structure in Figure 1) to further support our experimental measurements and assignments of Nor-Pt. Calculated spectra with absorption due to radiation polarized along the molecule (gray solid line) and the isotropic average of the absorption (black solid line) are presented in Figure 10A−D. The molecular coordinate systems, referring to the spectra in Figures 10A,D, are such that the *z*-direction is parallel with the surface normal of the respective aromatic ring. The coordinate system referring to the spectrum in Figure 10B is chosen so that the same molecular orientation is adopted as that for the molecular chain in Nor-Pt (the part of Nor-Pt synthesized from MPA). One implication of this choice is that spectral peaks for which the gray and black lines show a perfect overlap can be assigned to $\pi^*$ transitions, whereas a separation of lines indicate $\sigma^*$ character of the transition. We present the theoretically calculated spectrum for 3,4-dihydroxytoluene, in Figure 10A. Two 1s to $\pi^*$ transitions are clearly shown in the spectrum. The two peaks found at about 285.5 and 287.0 eV are assigned as the aromatic C−H and C−OH carbons, respectively. From our theoretical calculations we concluded that the peak at 285.5 eV is fully attributed to $\pi^*$ transitions in the aromatic ring, whereas the peak at 287.0 eV has mixed-in $\sigma^*$ character. The calculated C *K*-edge spectrum of 2-hydroxyethyl-3-mercaptoamide is presented in Figure 10B. The spectrum is dominated by a peak positioned at approximately 287.5 eV, which we assign to $\pi^*$(C═O) transitions in the amide moiety. This peak also has contribution from $\sigma^*$ transitions. The molecular building-block principle is illustrated in Figure 10, showing the sum of the calculated NEXAFS spectra of 3,4-dihydroxytoluene and 2-hydroxyethyl-3-mercaptoamide agrees well with the calculated NEXAFS spectrum of Nor-Pt; see Figure 10C,D.

One of our goals was to investigate the molecular orientation of Nor-Pt adsorbed onto gold substrate. The only

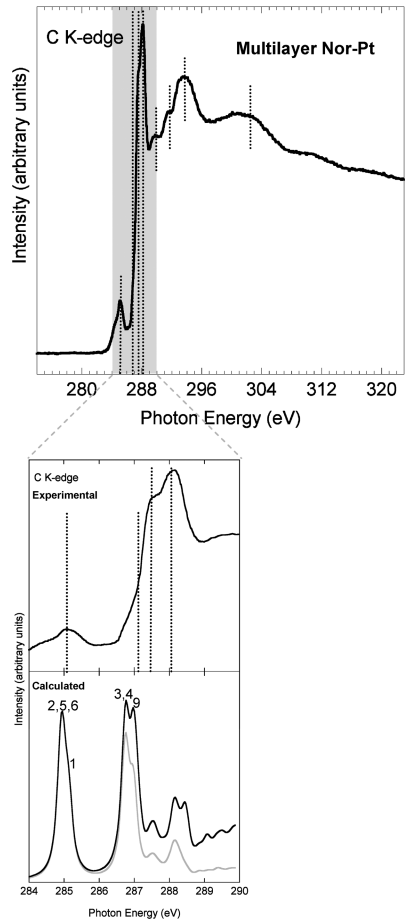


**Figure 8.** Carbon *K*-edge NEXAFS spectra of Nor-Pt in a multilayer form. The experimental spectrum is measured at an angle $\theta = 55°$ (the angle between the surface normal and the beam polarization). The enlargement includes a comparison with the corresponding theoretical spectrum.

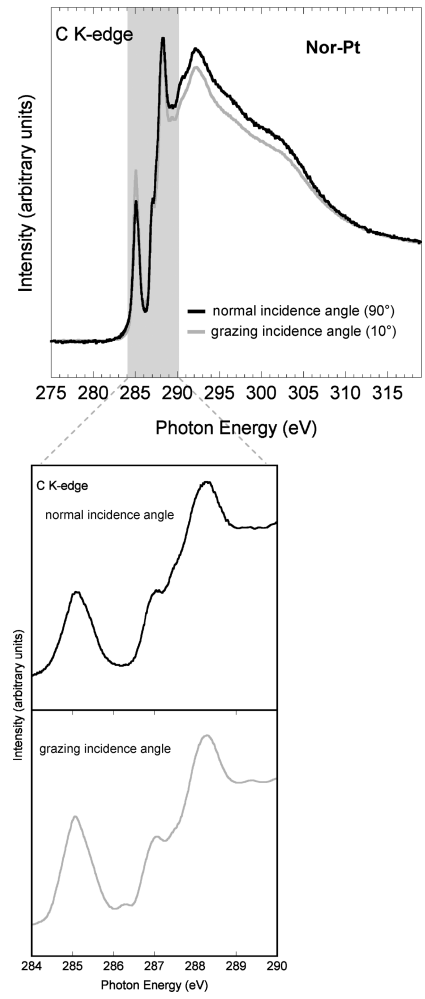


**Figure 9.** Experimental carbon *K*-edge NEXAFS spectra of a monolayer of Nor-Pt adsorbed on a Au(111) surface. The spectra are recorded at normal (solid black) and grazing (solid gray) incidence, which correspond to angles $\theta = 90$ and 10°, respectively (the angle between the surface normal and the beam polarization). The enlargement shows spectra at normal and grazing incidence individually.

peak with fully $\pi^*$ or $\sigma^*$ character was located at about 285 eV, and we used this peak to calculate the tilt angle of the aromatic ring. We conclude that we cannot use other resonances to estimate for example the tilt angle of the C═O $\pi^*$ orbital in the amide moiety as all other resonances have mixed $\pi^*$ and $\sigma^*$ character.

## 4. Conclusion

Multilayers of noradrenaline, multilayers of Nor-Pt, and monolayers of Nor-Pt on gold substrates have been characterized by means of chemical composition, the binding strength to the gold substrate, and the molecular orientation. The S 2p high-resolution XPS spectrum of the monolayer of Nor-Pt showed that the majority of Nor-Pt molecules have been chemisorbed to the gold surface. The orientation of the carbonyl group in the amide moiety of Nor-Pt could be determined with IR absorption spectroscopy. It is shown that the main component of the C═O vibrational modes is oriented parallel with respect to the gold surface. The peak positioned at approximately 285 eV in the C *K*-edge NEXAFS spectra of monolayers of Nor-Pt, which corresponds to C 1s to $\pi^*$ transitions of the aromatic carbons, was used to investigate the angle between the normal of the gold surface and the aromatic ring plane. We determine this angle to be equal to 51° for Nor-Pt monolayers on gold. It is shown that, for these types of molecular systems, the building block principle is a useful tool for detailed spectral analysis and assignments. Theoretical calculations were shown to be very useful for strengthen the assignments of angle dependent NEXAFS experimental data.

The Nor-Pt is clearly shown to adsorb to the gold substrate forming chemical bonds to the substrate and to organize with

**TABLE 4: Experimental Positions and Proposed Assignments of the Main Resonances Present in the C K-Edge NEXAFS Spectra of Noradrenaline and Nor-Pt**

| noradrenaline | mulitlayer Nor-Pt energy (eV) | monolayer Nor-Pt | assignment |
|---|---|---|---|
| 285.0 | 285.0 | 285.0 | C 1s → $\pi^*$ (C═C) |
| 286.7 | 287.1 | 287.0 | C 1s → $\pi^*$(C═C)[a] |
| | 287.5 | 287.8 | C 1s → $\pi^*$ (C═O)[b] |
| 288.1 | 288.1 | 288.4 | C 1s → $\pi^*$ (C═O)[c] |
| 290.0 | 290.0 | | C 1s → $\sigma^*$ (C—OH, C—N) |
| | 291.6 | 290.6 | C 1s → $\sigma^*$ (C—C) |
| 294 | 293 | 292 | C 1s → $\sigma^*$ (C—C, C—N) |
| 303 | 303 | 303 | C 1s → $\sigma^*$ (C═C, C═O) |

[a] The hydroxyl carbons in the aromatic ring (C—OH). [b] The carbonyl carbon in the amide moiety (C═ONH). [c] The carboxyl carbons (C═OOH).

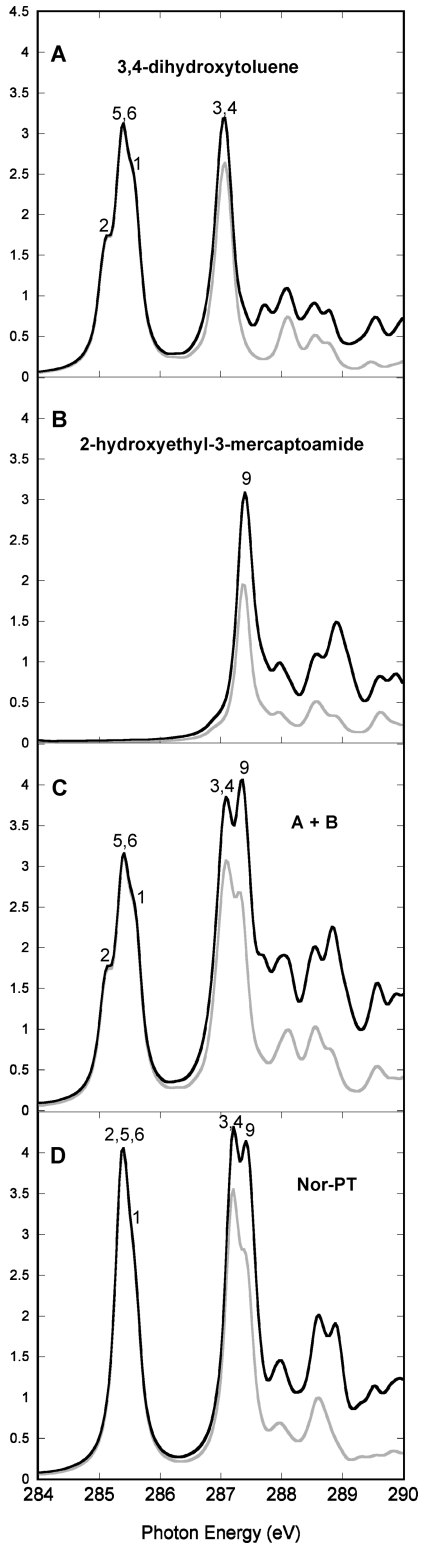


**Figure 10.** Theoretical carbon *K*-edge NEXAFS spectra of (A) 3,4-dihydroxytoluene, (B) 2-hydroxyethyl-3-mercaptoamide, (C) sum of spectra in panels A and B, and (D) Nor-Pt.

the aromatic ring available for molecular recognition. Mixed monolayers with passive molecular adsorbates would potentially even further increase the availability of the catechol group for further biointeraction.

**Acknowledgment.** This work was supported by grants from the Swedish Research Council (Grant No. 621-2007-5269 and Grant No. 621-2009-5148), VINNOVA (Grant No. 2009-00194) and Carl Tryggers Stiftelse (Grant No. 09:274 and Grant No. 09:390) as well as grant for computing time from National Supercomputer Centre (NSC), Sweden. We thank the MaxLab staff in Lund, and in particular the beamline manager for D1011 A. Preobrajenski, for assistance with our XPS and NEXAFS measurements.

## References and Notes

(1) McClary, K. B.; Ugarova, T.; Grainger, D. W. *J. Biomed. Mater. Res.* **2000**, *50*, 428–439.
(2) Spinke, J.; Liley, M.; Guder, H.-J.; Angermaier, L.; Knoll, W. *Langmuir* **1993**, *9*, 1821–1825.
(3) Prime, K. L.; Whitesides, G. M. *J. Am. Chem. Soc.* **1993**, *115*, 10714–10721.
(4) Ganong, W. F. *Review of Medical Physiology*, 20th ed.; Lange Medical Books/McGraw-Hill: New York, 2001.
(5) Clarke, S. J.; Hollmann, C. A.; Zhang, Z.; Suffern, D.; Bradforth, S. E.; Dimitrijevic, N. M.; Minarik, W. G.; Nadeau, J. L. *Nat. Mater.* **2006**, *5*, 409–417.
(6) Saifuddin, U.; Vu, T. Q.; Rezac, M.; Qian, H.; Pepperberg, D. R.; Desai, T. A. *J. Biomed. Mater. Res., Part A* **2003**, *66*, 184–191.
(7) Basti, H.; Tahar, L. B.; Smiri, L. S.; Herbst, F.; Vaulay, M.-J.; Chau, F.; Ammar, S.; Benderbous, S. *J. Colloid Interface Sci.* **2010**, *341*, 248–254.
(8) Nehilla, B. J.; Popat, K. C.; Vu, T. Q.; Chowdhury, S.; Standaert, R. F.; Pepperberg, D. R.; Desai, T. A. *Biotechnol. Bioeng.* **2004**, *87*, 669–674.
(9) Yan, C.; Matsuda, W.; Pepperberg, D. R.; Zimmerman, S. C.; Leckband, D. E. *J. Colloid Interface Sci.* **2006**, *296*, 165–177.
(10) Uvdal, K.; Ekeroth, J.; Konradsson, P.; Liedberg, B. *J. Colloid Interface Sci.* **2003**, *260*, 361–366.
(11) Petoral, R. M.; Uvdal, K. *J. Electron Spectrosc. Relat. Phenom.* **2003**, *128*, 159–164.
(12) Petoral, R. M.; Uvdal, K. *J. Phys. Chem. B* **2003**, *107*, 13396–13402.
(13) Becke, A. D. *J. Chem. Phys.* **1993**, *98*, 5648–5652.
(14) Dunning, T. H., Jr. *J. Chem. Phys.* **1989**, *90*, 1007–1023.
(15) Norman, P.; Bishop, D. M.; Jensen, H. J. Aa.; Oddershede, J. *J. Chem. Phys.* **2001**, *115*, 10323–10334.
(16) Norman, P.; Bishop, D. M.; Jensen, H. J. Aa.; Oddershede, J. *J. Chem. Phys.* **2005**, *123*, 194103–194118.
(17) Frisch, M. J.; *Gaussian 03*, Revision B05; Gaussian: Pittsburgh, PA, 2003.
(18) Dalton, a molecular electronic structure program, release 2.0. See: http://www.kjemi.uio.no/software/dalton/dalton.html, 2005.
(19) Moulder, J. F.; Stickle, W. F.; Sobol, P. E.; Bomben, K. D. *Handbook of X-ray Photoelectron Spectroscopy*; Physical Electronics: Eden Prairie, MN, USA, 1995.
(20) Ishida, T.; Choi, N.; Mizutani, W.; Tokumoto, H.; Kojima, I.; Azehara, H.; Hokari, H.; Akiba, U.; Fujihira, M. *Langmuir* **1999**, *15*, 6799–6806.
(21) Castner, D. G.; Hinds, K.; Grainger, D. W. *Langmuir* **1996**, *12*, 5083–5086.
(22) Heister, K.; Zharnikov, M.; Grunze, M.; Johansson, L. S. O.; Ulman, A. *Langmuir* **2001**, *17*, 8–11.
(23) Cavalleri, O.; Oliveri, L.; Daccà, A.; Parodi, R.; Rolandi, R. *Appl. Surf. Sci.* **2001**, *175−176*, 357–362.
(24) Wagner, A. J.; Carlo, S. R.; Vecitis, C.; Fairbrother, D. H. *Langmuir* **2002**, *18*, 1542–1549.
(25) Zharnikov, M. *J. Electron Spectrosc. Relat. Phenom.* **2010**, *178−179*, 380–393.
(26) Watcharinyanon, S.; Puglia, C.; Göthelid, E.; Bäckvall, J.-E.; Moons, E.; Johansson, L. S. O. *Surf. Sci.* **2009**, *603*, 1026–1033.
(27) Uvdal, K.; Bodö, P.; Liedberg, B. *J. Colloid Interface Sci.* **1992**, *149*, 162–173.
(28) Vahlberg, C.; Petoral, R. M.; Lindell, C.; Broo, K.; Uvdal, K. *Langmuir* **2006**, *22*, 7260–7264.
(29) Petoral, R. M.; Uvdal, K. *Colloids Surf., B* **2002**, *25*, 335–346.
(30) Schoenfisch, M. H.; Pemberton, J. E. *J. Am. Chem. Soc.* **1998**, *120*, 4502–4513.
(31) Hutt, D. A.; Leggett, G. J. *J. Phys. Chem.* **1996**, *100*, 6657–6662.
(32) Willey, T. M.; Vance, A. L.; van Buuren, T.; Bostedt, C.; Terminello, L. J.; Fadley, C. S. *Surf. Sci.* **2005**, *576*, 188–196.
(33) Zubavichus, Y.; Zharnikov, M.; Shaporenko, A.; Fuchs, O.; Weinhardt, L.; Heske, C.; Umbach, E.; Denlinger, J. D.; Grunze, M. *J. Phys. Chem. A* **2004**, *108*, 4557–4565.
(34) Whelan, C. M.; Barnes, C. J.; Walker, C. G. H.; Brown, N. M. D. *Surf. Sci.* **1999**, *425*, 195–211.

(35) Iucci, G.; Battocchio, C.; Dettin, M.; Gambaretto, R.; Polzonetti, G. *Surf. Interface Anal.* **2008**, *40*, 210–214.
(36) Simmons, N. J.; Aileen Chin, K. O.; Harnisch, J. A.; Vaidya, B.; Trahanovsky, W. S.; Porter, M. D.; Angelici, R. J. *J. Electroanal. Chem.* **2000**, *482*, 178–187.
(37) Baio, J. E.; Weidner, T.; Brison, J.; Graham, D. J.; Gamble, L. J.; Castner, D. G. *J. Electron Spectrosc. Relat. Phenom.* **2009**, *172*, 2–8.
(38) Pale-Grosdemange, C.; Simon, E. S.; Prime, K. L.; Whitesides, G. M. *J. Am. Chem. Soc.* **1991**, *113*, 12–20.
(39) Enkvist, C.; Lunell, S.; Svensson, S. *Chem. Phys.* **1997**, *214*, 123–130.
(40) Briggs, D.; Beamson, G. *Anal. Chem.* **1992**, *64*, 1729–1736.
(41) Palop, S. G.; Romero, A. M.; Calatayud, J. M. *J. Pharm. Biomed. Anal.* **2002**, *27*, 1017–1025.
(42) Vance, A. L.; Willey, T. M.; Nelson, A. J.; van Buuren, T.; Bostedt, C.; Terminello, L. J.; Fox, G. A.; Engelhard, M.; Baer, D. *Langmuir* **2002**, *18*, 8123–8128.
(43) Bain, C. D.; Troughton, E. B.; Tao, Y.-T.; Evall, J.; Whitesides, G. M.; Nuzzo, R. G. *J. Am. Chem. Soc.* **1989**, *111*, 321–335.
(44) Heister, K.; Zharnikov, M.; Grunze, M.; Johansson, L. S. O. *J. Phys. Chem. B* **2001**, *105*, 4058–4061.
(45) Ihs, A.; Liedberg, B. *J. Colloid Interface Sci.* **1991**, *144*, 282–292.
(46) Tengvall, P.; Lundström, I.; Liedberg, B. *Biomaterials* **1998**, *19*, 407–422.
(47) Podstawka, E.; Kafarski, P.; Proniewicz, L. M. *J. Phys. Chem A* **2008**, *112*, 11744–11755.
(48) Ayala, I.; Range, K.; York, D.; Barry, B. A. *J. Am. Chem. Soc.* **2002**, *124*, 5496–5505.
(49) Izgi, T.; Alver, Ö.; Parlak, C.; Aytekin, M. T.; Senyel, M. *Spectrochim. Acta, Part A* **2007**, *68*, 55–62.
(50) Jung, C. *J. Mol. Recognit.* **2000**, *13*, 325–351.
(51) Stohr, J. *NEXAFS Spectroscopy*; Springer: Berlin, 1992.
(52) Villaume, S.; Norman, P. *Chirality* **2009**, *21*, S13–S19.
(53) Kaznacheyev, K.; Osanna, A.; Jacobsen, C.; Plashkevych, O.; Vahtras, O.; Ågren, H.; Carravetta, V.; Hitchcock, A. P. *J. Phys. Chem. A* **2002**, *106*, 3153–3168.
(54) Francis, J. T.; Hitchcock, A. P. *J. Phys. Chem.* **1992**, *96*, 6598–6610.
(55) Zubavichus, Y.; Shaporenko, A.; Grunze, M.; Zharnikov, M. *J. Phys. Chem. A (Lett.)* **2005**, *109*, 6998–7000.
(56) Zubavichus, Y.; Zharnikov, M.; Schaporenko, A.; Grunze, M. *J. Electron Spectrosc. Relat. Phenom.* **2004**, *134*, 25–33.
(57) Cooper, G.; Gordon, M.; Tulumello, D.; Turci, C.; Kaznatcheev, K.; Hitchcock, A. P. *J. Electron Spectrosc. Relat. Phenom.* **2004**, *137−140*, 795–799.

JP105696J